Quantized vortices in dipolar supersolid Bose-Einstein-condensed gases

A. Gallemí, S. M. Roccuzzo, S. Stringari, and A. Recati*
INO-CNR BEC Center and Dipartimento di Fisica, Università degli Studi di Trento, 38123 Povo, Italy and Trento Institute for Fundamental Physics and Applications, INFN, 38123, Trento, Italy

(Received 13 May 2020; accepted 7 July 2020; published 21 August 2020)

We investigate the properties of quantized vortices in a dipolar Bose-Einstein condensed gas by means of a generalized Gross-Pitaevskii equation. The size of the vortex core hugely increases by increasing the weight of the dipolar interaction, approaching the transition to the supersolid phase. The critical angular velocity for the existence of an energetically stable vortex decreases in the supersolid, due to the reduced value of the density in the interdroplet region. The angular momentum per particle associated with the vortex line is shown to be smaller than $\hbar$, reflecting the reduction of the global superfluidity. The real-time vortex nucleation in a rotating trap is shown to be triggered, as for a standard condensate, by the softening of the quadrupole mode. For large angular velocities, when the distance between vortices becomes comparable to the interdroplet distance, the vortices are arranged into a honeycomb structure, which coexists with the triangular geometry of the supersolid lattice and persists during the free expansion of the atomic cloud.

DOI: 10.1103/PhysRevA.102.023322

I. INTRODUCTION

The recent realization of supersolidity in dipolar Bose-Einstein condensed gases [1–3] is stimulating novel experimental and theoretical work aimed at studying the superfluid properties of these intriguing systems, which exhibit the spontaneous breaking of both gauge and translational symmetry yielding superfluidity and crystal periodic order, respectively (see, e.g., Refs. [4–7]). Experimental evidence of phase coherence among the droplets forming the crystal structure [1–3], the occurrence of Goldstone modes associated with the spontaneous breaking of both symmetries [8–10], and the reduction of the moment of inertia with respect to the rigid value [11] have provided important signatures of the superfluid behavior of these systems. Conclusive proof of superfluidity is, however, given by the observation of quantized vortex lines, following the seminal papers of Refs. [12–16] in Bose-Einstein condensates and strongly interacting Fermi gases, respectively. The realization of quantized vortices, hosted by the crystal configuration of the supersolid, then represents a challenging task to pursue. This possibility, so far not yet experimentally realized, has been the object of recent theoretical investigations [17]. Even the structure of quantized vortices in the fully superfluid phase and, in particular, the effect of the long-range dipolar force on the size of the vortex core and on the value of the critical angular velocity needed to ensure the energetic stability of a single vortex line, represents an interesting topic, hopefully of near-future experimental investigation. The purpose of this paper is to provide a comprehensive theoretical investigation of the structure of quantized vortices in a Bose-Einstein condensate characterized by a long-range dipolar interaction with special focus on the supersolid phase.

Our investigation is based on the use of a suitable extension of the Gross-Pitaevskii equation to include the beyond mean-field term (see Sec. II) in the equation of state accounting for quantum fluctuations [18], which plays a crucial role in the emergence of supersolidity and the formation of self-bound droplets (see Fig. 1). In Sec. III, we explore the properties of a single vortex line in both the superfluid and the supersolid case. In the superfluid phase, the dipolar interaction hugely increases the vortex core size as compared to Bose gases with only zero-range interaction. In the supersolid phase, vortices are hosted in the region separating the droplets forming the crystal structure and their shape is strongly deformed by the presence of the droplets. We show that the value of the critical angular velocity exhibits an important reduction by increasing the ratio between the dipolar and the zero-range strengths of the interatomic force. Furthermore, we show that the angular momentum carried by a vortical line in an axisymmetrically trapped supersolid is reduced with respect to the usual value $\hbar$ as a consequence of the reduced superfluidity of the system. By carrying out a time-dependent simulation, we also point out that the nucleation process for the creation of a vortical line in the supersolid phase is favored by the softening of the quadrupole mode frequency. In Sec. IV, we study the case of higher angular velocities and show that the coexistence of the density modulation and vorticity yields a honeycomb vortex lattice in place of the usual triangular (Abrikosov) lattice, the coexistence persisting during the expansion following the sudden release of the trap. We sum up our conclusions in Sec. VI.

II. DIPOLAR GROSS-PITAEVSKII EQUATION WITH LEE-HUANG-YANG CORRECTION

We consider a dipolar Bose gas of ^{164}Dy atoms trapped by an in-plane isotropic harmonic potential $V_{\rm ho}(\mathbf{r}) = \frac{1}{2}m\omega^2(x^2 + y^2 + \lambda^2 z^2)$, with $\lambda = \omega_z/\omega$, and m the atomic mass. At zero

*Corresponding author: alessio.recati@ino.it

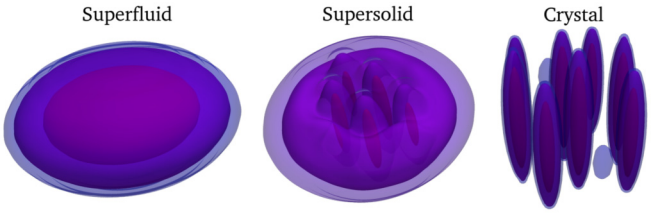

FIG. 1. Example of the three distinct phases of a dipolar Bose gas in a pancake geometry (from left to right): superfluid, supersolid, and droplet crystal phase. The pictures are obtained as ground-state solutions of the extended Gross-Pitaevskii Eq. (1) for 10^5 atoms by decreasing the s-wave scattering length to favor the long-range anysotropic dipolar interaction (see text).

temperature, the gas can be characterized by a single macroscopic wave function $\Psi(\mathbf{r}, t)$, whose temporal evolution is described by a generalized Gross-Pitaevskii equation. The latter takes into account the contact, the dipole-dipole interaction, and the quantum fluctuations [19] and can be written as

$$i\hbar\frac{\partial}{\partial t}\Psi(\mathbf{r}, t) = \mathcal{H}(\mathbf{r})\,\Psi(\mathbf{r}, t)\,, \tag{1}$$

where the Hamiltonian is

$$\mathcal{H}(\mathbf{r}) = -\frac{\hbar^2}{2m}\nabla^2 + V_{\rm ho}(\mathbf{r}) + g|\Psi(\mathbf{r}, t)|^2 + \gamma(\varepsilon_{dd})|\Psi(\mathbf{r}, t)|^3 + \int d\mathbf{r}' V_{dd}(\mathbf{r}-\mathbf{r}')|\Psi(\mathbf{r}', t)|^2\,, \tag{2}$$

with $g = 4\pi\hbar^2 a/m$ the coupling constant fixed by the s-wave scattering length a and $V_{dd}(\mathbf{r}_i - \mathbf{r}_j) = \frac{\mu_0\mu^2}{4\pi}\frac{1-3\cos^2\theta}{|\mathbf{r}_i-\mathbf{r}_j|^3}$ the dipole-dipole potential, μ_0 being the magnetic permeability in vacuum, μ the magnetic dipole moment, and θ the angle between the vector distance between dipoles and the polarization direction, which we choose as the z axis. In the absence of trapping, the system can be fully characterized by the single parameter $\varepsilon_{dd} = \mu_0\mu^2/(3g) = a_{dd}/a$, i.e., the ratio between the strength of the dipolar and the contact interaction, eventually written in terms of the dipolar length a_{dd} and the scattering length a. For the atom we are using, $a_{dd} = 131\,a_B$, where a_B is the Bohr radius. The third term of the Hamiltonian Eq. (2) corresponds to the local density approximation of the beyond-mean-field Lee-Huang-Yang (LHY) correction [18,20], with

$$\gamma(\varepsilon_{dd}) = \frac{16}{3\sqrt{\pi}}ga^{\frac{3}{2}}\,\mathrm{Re}\left[\int_0^\pi d\theta\,\sin\theta[1+\varepsilon_{dd}(3\cos^2\theta-1)]^{\frac{5}{2}}\right]. \tag{3}$$

Experimental measurements and microscopic Monte Carlo calculations [21] have confirmed that the LHY term is an accurate correction to the mean-field theory given by the Gross-Pitaevskii equation both in dipolar gases and quantum mixtures [22–26]. At the mean-field level, increasing the role of the dipolar interaction would lead to the collapse of the cloud because of the attractive component of the dipolar force. The collapse is prevented by a strong confinement in the polarization direction z, ($\lambda \gg 1$) causing the occurrence of a typical rotonlike excitation spectrum [27], whose gap becomes smaller and smaller as one increases ϵ_{dd}, and by the inclusion of the LYH term. Both effects are responsible for the emergence of new interesting phases. In particular, a dipolar Bose gas confined in the polarization direction has been shown to be fully superfluid for a value of ε_{dd} lower than a certain critical value of the order of 1.3 (this value has a weak dependence on the trapping parameters and the total atom number N). Above this value, that would correspond to a roton collapse in the absence of the LHY effect, the system presents supersolid properties characterized by density modulations and coherence between the density peaks. Further increasing ε_{dd}, the system enters the crystal phase, where coherence between the density peaks is destroyed and global superfluidity is lost.

In Ref. [17], we have recently shown that supersolids are able to host quantized vortices in the low-density region between the density peaks, with a deformed vortex core. In the following, we determine the behavior of the relevant properties of these vortices by changing the value of the relevant parameter ε_{dd}.

To study vortices, we add to the Hamiltonian of the system the angular momentum constraint $-\Omega L_z$, where L_z is the angular momentum operator and Ω is the angular rotation frequency, and solve the Gross-Pitaevskii equation either in imaginary or real time as explained in detail in the following. In particular, the ground state of a superfluid is insensible to rotations for Ω lower than a critical value Ω_c, above which the presence of a vortex in the system becomes energetically favorable. The new stable vortical configuration carries an angular momentum per particle equal to $\hbar$. Supersolids, instead, react to any value of the angular frequency due to the existence of a nonsuperfluid component [17] and for the same reason, the angular momentum carried by a vortex line is expected to be smaller than the usual value $\hbar$, as we explicitly verify in the next section.

III. SINGLE VORTEX LINE

In this section, we analyze the properties of a single vortex line oriented along the z direction and located in the center of the trap. We present the results for its core size, its energy, and its angular momentum across the superfluid-supersolid transition. Furthermore, we show that, similarly to the case of usual superfluids [28,29], the nucleation of vortices in a rotating trap, is dictated by the quadrupole deformation of the superfluid component.

A. Vortex core structure

The structure of the vortex core in superfluids is deeply connected to a length called healing length. In condensates with only contact interactions, the healing length is computed as the half width half maximum of the wave function. Keeping the same definition as valid for the dipolar case, seminal papers already studied in detail the dependence of the healing length on the scattering length for dipolar gases without the LHY correction [30,31]. In these works, it has been shown that the healing length of the vortex increases by increasing $\varepsilon_{\rm dd}$ until the gas collapses.

As mentioned above, quantum fluctuations prevent the collapse, and the supersolid phase emerges in the trapped geometry at higher values of ϵ_{dd}. In Fig. 2, we report the

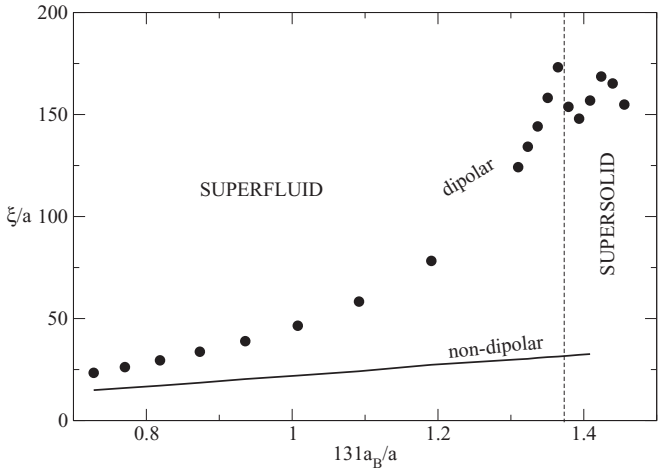

FIG. 2. Healing length defined as the vortex core size (see text) as a function of the scattering length a by crossing the superfluid to supersolid transition, both in the nondipolar (solid line) and dipolar (points) case.

healing length as the system goes from the superfluid into the supersolid regime, by solving in imaginary time the Gross-Pitaevskii equation in a rotating frame with angular frequency Ω. We find that the healing length keeps increasing till the transition point, after which a nonmonotonic and irregular behavior is observed. At the transition point, there appears to be a jump. In the supersolid phase, the healing length does not show a monotonic behavior but it remains roughly constant. As noticed already in Ref. [17], indeed, in the supersolid phase the vortex core size is of the same order of the peak density distance, which implies that the vortex core is no longer characterized by atom-atom interactions but deeply modified by the crystal structure. The healing length for the nondipolar case is also shown for comparison.

B. Critical rotation frequency

The vortex line previously described is energetically stable only above a certain angular frequency Ω_c, which makes the energy in the rotating frame of the system with the vortex lower than the energy without the vortex. We have calculated the value of the critical rotation frequency for a stable vortex line in the center as a function of ε_{dd} across the superfluid-supersolid-crystal transition, shown in Fig. 3(a). There are already several works [30–32] accounting for the dependence of the critical rotation frequency as a function of ε_{dd} in dipolar condensates without including quantum fluctuations. In that case, Ω_c increases with ε_{dd}, reaching a maximum for $\varepsilon_{dd} = 1$, and decreasing for larger values until the collapse is achieved. Thanks to the inclusion of the beyond-mean-field term in the Gross-Pitaevskii equation one can go beyond the mean-field collapse, eventually entering the supersolid phase. We find that after the maximum is reached, the critical frequency keeps decreasing, showing a rather small jump at the transition to the supersolid regime, and continues decreasing until the crystal phase is reached.

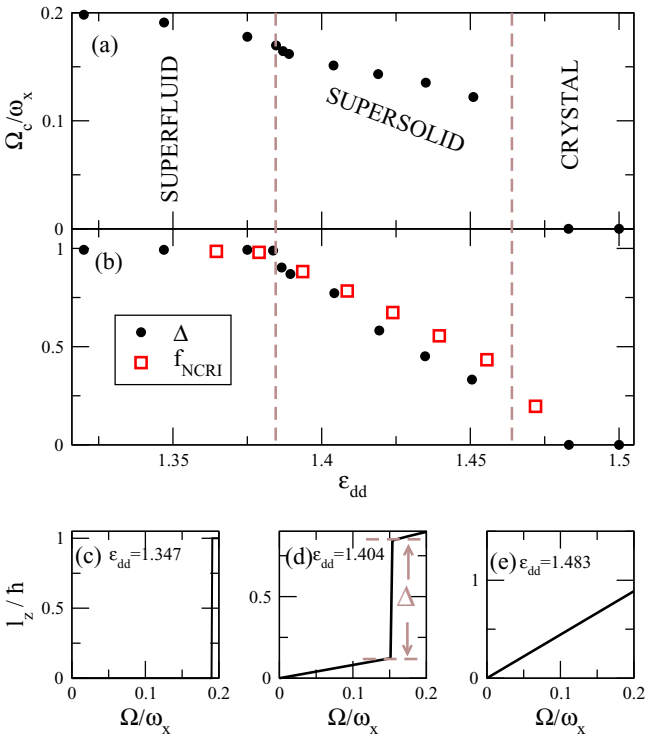

FIG. 3. (a) Critical rotation frequency as a function of ε_{dd}. (b) Jump of the angular momentum Δ and nonclassical momentum of inertia fraction f_{NCRI} as a function of ε_{dd}. Angular momentum as a function of the rotation frequency Ω for (c) $\varepsilon_{dd} = 1.347$, (d) $\varepsilon_{dd} = 1.404$, and (e) $\varepsilon_{dd} = 1.483$, respectively, in the superfluid, supersolid, and crystal regimes. The other parameters are $N = 40\,000$ atoms and trapping frequencies $\omega_{x,y,z} = 2\pi \times (60, 60, 120)$ Hz.

C. Angular momentum carried by a vortex

In a fully superfluid system, the angular momentum per particle carried by a vortex line is $\hbar$. In a partially superfluid system, this value should instead become smaller. The angular momentum carried by the vortex corresponds to the jump $\Delta\hbar$ in the angular momentum per particle at $\Omega = \Omega_c$ by increasing the angular velocity from below to above the critical value. We have determined such a jump across the whole zero-temperature phase diagram of the trapped dipolar gas and the value of Δ is reported in Fig. 3(b). As intuitively expected, we find that $\Delta = 1$ in the superfluid phase, it decreases monotonically in the supersolid phase and eventually becomes zero in the droplet crystal phase. For completeness, the angular momentum per particle as a function of Ω is reported in Figs. 3(c)–3(e), corresponding to the superfluid, supersolid, and droplet crystal regime, respectively.

It is interesting to analyze the connection between Δ and the superfluid fraction of the system through the jump in the moment of inertia. Such a jump is only due to the presence of a superfluid part in a supersolid, and therefore Δ itself is a natural quantity to evaluate the global superfluidity of the system. Another very relevant quantity to characterize the superfluidity of finite systems is the nonclassical rotation of inertia fraction that we studied in detail for the dipolar supersolid gas in Ref. [17]. The nonclassical rotation of inertia

fraction is given by

$$f_{\mathrm{NCRI}} = 1 - \Theta/\Theta_{\mathrm{rig}}\,, \tag{4}$$

where Θ is the moment of inertia of the system and Θ_{rig} is its rigid body value. As pointed out by Leggett [33] in cylindrical annulus, f_{NCRI} coincides with the superfluid fraction f_s. In Fig. 3(b), we compare f_{NCRI} and Δ. In the superfluid phase, they are both equal to 1, i.e., the whole system is superfluid. In the supersolid region, they start deviating from each other with $f_{\mathrm{NCRI}} > \Delta$. In the droplet crystal phase, f_{NCRI} remains finite, while $\Delta = 0$. The reason is due to the fact that each density peak (droplet) in the crystal phase is superfluid by itself, therefore increasing the value of the nonclassical rotation of inertia. On the other hand, Δ only accounts for the superfluid component participating in the rotation due to the presence of a vortex.

D. Quadrupole instability and vortex nucleation

In this section, we address the problem of vortex nucleation by rotating the harmonic trap, as implemented almost 20 years ago for a standard ^{87}Rb BEC [29]. The dynamics of vortex nucleation in ordinary (nondipolar) condensates in a rotating trap has been extensively studied. Vortex nucleation is induced by the introduction of a suitable rotating deformation of the trap, characterized by a rotation frequency Ω and deformation parameter $\epsilon = (\omega_x^2 - \omega_y^2)/(\omega_x^2 + \omega_y^2)$.

It turns out that there indeed exists a critical frequency for vortex nucleation Ω_{vn} [13,29], which is significantly higher than the one at which a vortex becomes energetically favorable. The reason is due to the presence of an energetic barrier [34] for the vortex to enter due to the need of creating a density depletion at the vortex position. In Refs. [28,35], it was shown that for rotating harmonic traps, the mechanism of vortex nucleation is triggered by the dynamic instability of the quadrupole mode, according to the resonance condition

$$\Omega_{\mathrm{vn}} = \omega_q/2\,, \tag{5}$$

with $\omega_q = \sqrt{2}\,\omega_\perp$ the frequency of the quadrupole mode in the absence of rotation [36]. The dynamical instability leads to the spontaneous breaking of the cylindrical symmetry of the cloud creating the condition for vortices to be nucleated [28,35].

Not surprisingly, considering the Gross-Pitaevskii equation without the LHY term, dipolar superfluids show the same kind of quadrupole instability [30,37], which could therefore drive vortex nucleation, when the resonance condition is satisfied. Notice, however, that for a dipolar gas, the quadrupole frequency ω_q is not simply given by $\sqrt{2}\omega_\perp$ but it depends on the interaction strength and the trapping parameters of the dipolar gas (see, e.g., Ref. [37]). Quite remarkably, by direct numerical simulations, we have shown that the critical frequency for the vortex nucleation is still given by the resonant condition Eq. (5) also when the LHY correction is included and even when the system is in the supersolid phase.

We consider $N = 40\,000$ atoms confined in a harmonic trap with frequencies $\omega_{x,y,z} = 2\pi \times (60, 60, 120)$ Hz, whose ground state configuration is obtained by propagation in imaginary time of Eq. (1). The quadrupole mode frequency of the system is obtained by evolving the system in real time under the action of a small, sudden quadrupolar deformation of the trap. We find that a sudden quadrupolar perturbation in the supersolid phase excites three modes that can be associated with the three Goldstone modes expected for an infinite, quasi-2D supersolid [4,38]: one Goldstone mode associated with the spontaneous breaking of the U(1) symmetry responsible for superfluidity and two associated with the spontaneous breaking of translational invariance along two directions. The results for the quadrupole frequencies are reported in Fig. 4. They extend to the 2D case our previous findings for the axial breathing mode of an elongated system [8]. As expected, we find that the lower mode decreases as ϵ_{dd} is increased, being dominated by the (global) superfluidity of the system, which disappears approaching the droplet crystal phase. The other two frequencies, dominated by the motion of the crystal peaks, increase until saturation in analogy to what we found in Ref. [8].

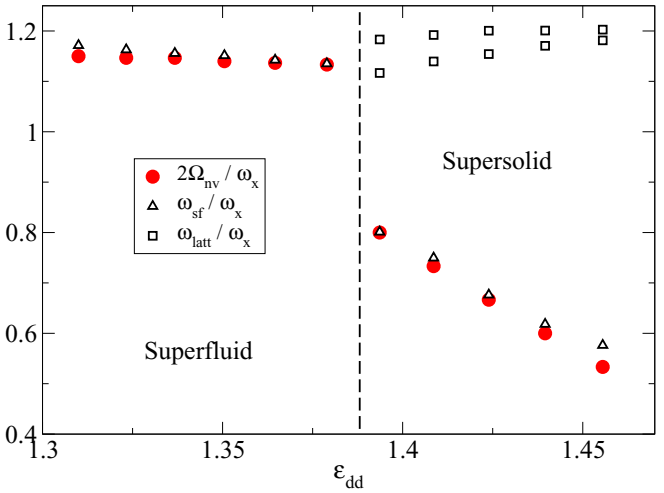

FIG. 4. Twice the critical frequency for vortex nucleation via the introduction of a rotating quadrupolar deformation (red circles), and frequencies of quadrupolar compressional modes (empty symbols), as a function of ϵ_{dd}. While in the superfluid phase, one finds a single mode excited by a sudden quadrupolar deformation (triangles), in the supersolid phase one finds three modes, two of which are associated with lattice excitations (empty squares) and one with superfluid oscillations (triangles), reflecting the presence of three Goldstone modes in an infinite system. The relation $\Omega_c = \omega_{q,sf}/2$, expected for a superfluid, remains valid also in the supersolid.

The nucleation of the vortex is studied instead by evolving Eq. (1) in real time starting from the ground state by adding the $-\Omega L_z$ term to the Hamiltonian [39]. A very small trap deformation ($\epsilon = 3.33 \times 10^{-3}$) to trigger the instability is also added. We observe that for any value of ε_{dd} there exists a critical angular frequency Ω_{vn}, such that for $\Omega \geqslant \Omega_{\mathrm{vn}}$ strong cloud deformations occur followed by the nucleation of a vortex (see Fig. 5) [40]. In Fig. 4, we report the calculated values of Ω_{vn} multiplied by a factor of 2 to make the comparison with the lowest quadrupole frequency more direct and explicit. The resonance condition Eq. (5) considering the (superfluid) lower frequency mode is met.

A comment on the timescale for vortex nucleation is due here. Our simulation predicts rather long times (of the order of 1 second) for the vortex nucleation at $T = 0$. However,

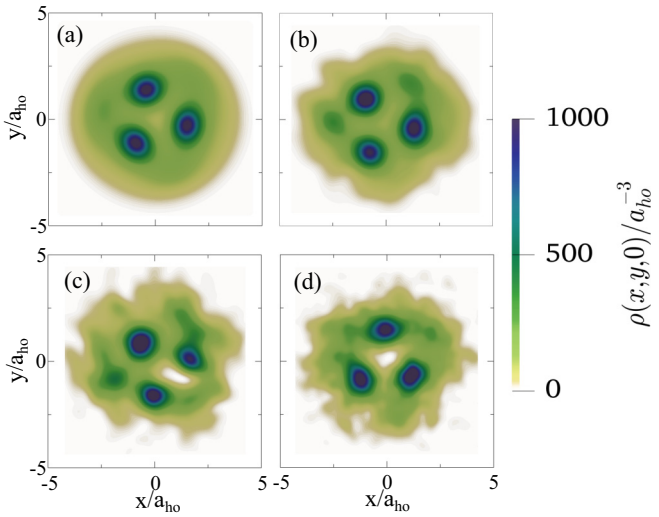

FIG. 5. *In situ* density profiles along the $z = 0$ plane showing the nucleation of a vortex in a gas of $N = 40\,000$ ^{164}Dy atoms in a slightly deformed trap, of frequencies $\omega_{x,y,z} = 2\pi \times (59.9, 60.1, 120)$ Hz and $\epsilon_{dd} = 1.394$. (a) Initial preparation of the gas in the supersolid ground state. (b) The system is put in rotation by the adiabatic introduction of an angular momentum constraint, until the angular velocity of $2\pi \times 20$ Hz is reached. The system shows a slight quadrupolar deformation in the $z = 0$ plane. Several vortices forms at the surface of the system. (c) The vortices try to penetrate the lattice through the interstitial region between the droplets to lower the energy. (d) A single vortex finally settles in the middle of the trap.

in real experiments, noise and thermal effects are expected to trigger the instability on a much faster timescale, since noise accelerates the spontaneous breaking of the cylindrical symmetry of the cloud [41]. Moreover, the presence of the thermal cloud, which exchanges energy with the condensate, favors the relaxation process through which the vortex lattice settles. We also checked that, as expected, larger, yet small, trap deformations help in speeding up the nucleation process. For instance, increasing ϵ of an order of magnitude ($\epsilon \simeq 0.03$) reduces the time for the vortex nucleation of also an order of magnitude $\simeq 100$ ms.

IV. VORTEX LATTICES IN DIPOLAR SUPERSOLIDS

A superfluid can host more than a single vortex line, if the rotational frequency is large enough. Many vortices form in the $z = 0$ plane, a 2D triangular lattice called *Abrikosov lattice* [14,15]. The aim of this section is to address the question of whether and how a dipolar supersolid can host many vortices. The presence of the regular (triangular lattice) density modulation can indeed interfere with the formation of the Abrikosov lattice, when the intervortex distance (which scales as $\Omega^{-1/2}$) becomes of the same order of the distance between the density peaks (the latter being fixed by the roton wave vector [27], which in supersolids is of the order of a few units of the axial oscillator length $\sqrt{\hbar/m\omega_z}$).

We have first checked that the triangular Abrikosov lattice persists in the whole superfluid regime, also in the presence of the dipolar interaction and LHY term, till the transition to the supersolid phase [42].

In the supersolid phase, it is energetically favorable to accommodate the vortices in the low density regions. Therefore, when the vortex distance is of the same order of the distance between the density peaks, there is a competition between the natural tendency of vortices forming the triangular Abrikosov lattice and the vortices occupying the valleys of the supersolid density. In Fig. 6(b), we show the numerical result of the imaginary-time evolution of the extended Gross-Pitaevskii equation in a rotating frame for large enough angular velocities. We obtain that the vortices are pinned by the minima of the supersolid density modulations forming—for the choosen value $\Omega = 2/3\,\omega_\perp$—a honeycomb lattice. It is instructive to compare it with the system for $\Omega = 0$, reported in Fig. 6(a). The increase of the cloud's radius (and the density reduction) due to the centrifugal potential allows a larger number of peaks to be hosted in the system.

It is important to notice that in the literature, the pinning of Abrikosov vortex lattices in Bose gases has been addressed by a number of authors considering an underlying (square or triangular) rotating optical lattice [43–46], with a nice early experimental demonstration of the transition from the "natural" Abrikosov lattice to the pinned vortex lattice by Eric Cornell and coworkers [47]. We remind the reader, however, that in our case, the structure of the density modulation is not imposed by an external potential but is due to the spontaneous

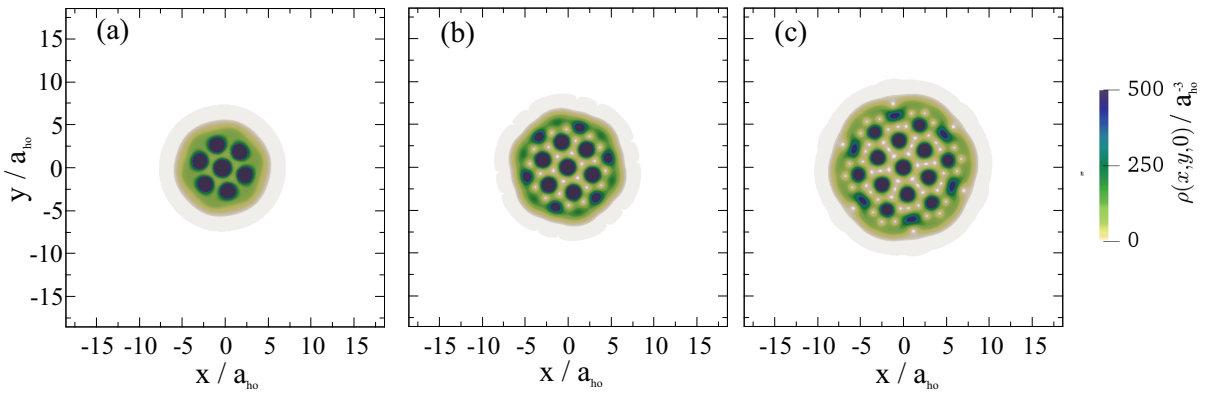

FIG. 6. Density plots of $N = 110\,000$ ^{164}Dy atoms in the supersolid phase for $\epsilon_{dd} = 1.409$, confined in an harmonic trap with frequencies $\omega_{x,y,z} = 2\pi \times (60, 60, 120)$ Hz. (a) Nonrotating gas $\Omega = 0$, (b) $\Omega = 2/5\omega_x$, and (c) $\Omega = 5/6\omega_x$.

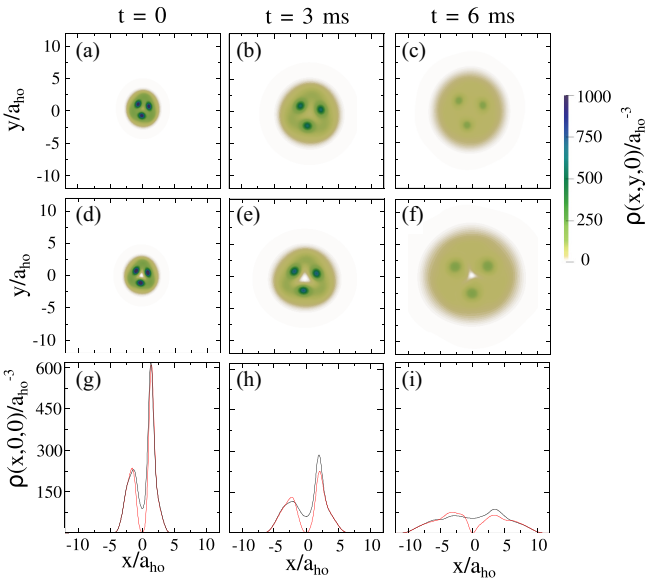

FIG. 7. *In situ* density profiles along the $z = 0$ plane [panels (a)–(f)], and cuts along the x axis [panels (g)–(i)] of an expanding dipolar supersolid in the absence [(a)–(c)] and presence [(d)–(f)] of a vortex. The initially prepared ground state in the presence (d) of a vortex has been obtained for $\Omega = 2\pi \times 20$ Hz. Panel (g) shows the corresponding density cut along the x axis. The red (black) line corresponds to the case with (without) vortex. Panels (h) and (i) show corresponding cuts along the x axis. The other parameters are the same as in Fig. 5. (A full movie of the expansion is available as Supplementary Material [40].)

breaking of translational symmetry, yielding the supersolid phase.

The pinned honeycomb lattice persists as long as Ω is not too large for the intervortex distance to become smaller than the period of the supersolid lattice. By further increasing Ω, we find that the vortices are hosted in the low density regions surrounding the droplets as shown in Fig. 6(c) for $\Omega = 5/6\,\omega_\perp$.

V. EXPANDING A SUPERSOLID WITH VORTEX LINES

The previously reported results considered the possibility of addressing the system *in situ*. Here we briefly discuss the effect of letting the cloud expand, i.e., after switching off the trap in the transverse ($z = 0$) plane to image the system with a better space resolution. We consider both the single and the many-vortex case.

Figure 7 shows the density profiles of a dipolar supersolid with and without a vortex line at two different times after the removal of the trap [40]. The ratio between the peak density and the central density, in the absence of the vortex, is less than 10 and it further decreases during the expansion, the minimum of the density remaining of the same order as that of an ordinary superfluid. Thus, with our choice of parameters, a good imaging system could easily identify the presence of the vortex in the center of the trap.

For the high angular frequency case, when many vortices appear, we consider the most interesting case, when the vortices form a honeycomb lattice, as in Fig. 6(b). The expansion at two different times after switching off the transverse confinement is reported in Fig. 8 [40]. In particular, we notice that the geometry of the two lattices remains unchanged during the expansion, paving the way for the possible direct observation of the frustration of the vortex lattice.

Concerning the latter case, we recently became aware of a very recent work [48] discussing a protocol to produce a vortex lattice in a large supersolid cloud and exploring the following dynamics of the expansion.

VI. CONCLUSIONS

In this paper, we have provided a comprehensive study of quantized vortex lines in the supersolid phase of an ultracold dipolar gas rotating in the plane orthogonal to the polarization direction of the dipole moment of the atoms. The analysis has been carried out by means of the generalized Gross-Pitaevskii equation [Eqs. (1) and (2)], including LHY corrections for the stabilization of the supersolid phase.

We have studied in detail the stationary properties and the nucleation dynamics of a single vortex line hosted in the

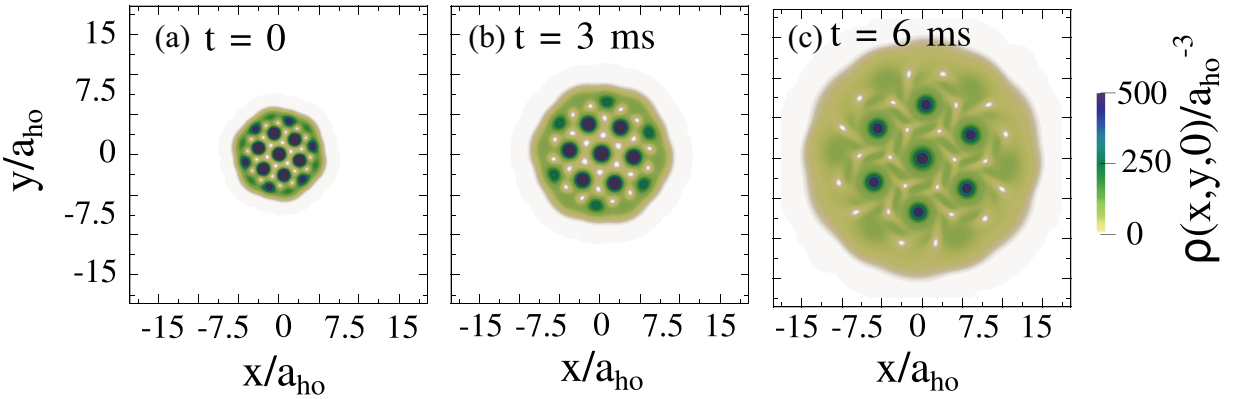

FIG. 8. Expansion of a dipolar supersolid in the presence of the vortex lattice reported in Fig. 6(b). (a) The initially prepared ground state. This state is evolved in real time, after switching off the radial confinement. Panels (b) and (c) show the $z = 0$ density profile at two later times (A full movie of the expansion is available as Supplementary Material [40].)

center of the cloud. We have found that the width of the vortex lines, close and in the supersolid phase, is significantly larger than in usual condensates interacting with contact forces. The width is large enough to be likely directly imaged with available *in situ* techniques. The critical rotational frequency for the energetic stability of a vortex has been found to decrease by increasing the dipolar interaction strength close to and into the supersolid phase. The angular momentum carried by a vortex is smaller than $\hbar$ in the supersolid phase and approaches zero by approaching the crystal droplet phase due to the reduction of the superfluid density of the cloud. Remarkably, we could show that the nucleation of a vortex is always triggered by the softening of the lowest quadrupole mode frequency (see Fig. 4), as in standard Bose-Einstein condensates with contact interaction.

At large enough angular velocity, we have addressed the problem of the spatial arrangement of many vortices. The supersolid phase forces the vortices to be pinned in the density valleys. In particular, we have shown that vortices arrange in a regular honeycomb lattice when the intervortex distance is of the same order of the solid periodicity [Fig. 6(b)], the supersolid vortex structure being preserved during the free expansion, following the release of the trap.

ACKNOWLEDGMENTS

Useful discussions with Franco Dalfovo, Giacomo Lamporesi and with the members of the Ferlaino's Dipolar Quantum Gas group are acknowledged. This project has received funding from the European Union's Horizon 2020 research and innovation program under Grant Agreement No. 641122 QUIC, from Provincia Autonoma di Trento, the Q@TN initiative and the FIS$\hbar$ project of the Istituto Nazionale di Fisica Nucleare.

[1] L. Tanzi, E. Lucioni, F. Famà, J. Catani, A. Fioretti, C. Gabbanini, R. N. Bisset, L. Santos, and G. Modugno, Phys. Rev. Lett. **122**, 130405 (2019).
[2] F. Böttcher, J.-N. Schmidt, M. Wenzel, J. Hertkorn, M. Guo, T. Langen, and T. Pfau, Phys. Rev. X **9**, 011051 (2019).
[3] L. Chomaz, D. Petter, P. Ilzhöfer, G. Natale, A. Trautmann, C. Politi, G. Durastante, R. M. W. van Bijnen, A. Patscheider, M. Sohmen *et al.*, Phys. Rev. X **9**, 021012 (2019).
[4] A. F. Andreev and I. M. Lifshitz, Zh. Eksp. Teor. Fiz. **56**, 2057 (1969) [Sov. Phys. JETP **29**, 1107 (1969)].
[5] D. T. Son, Phys. Rev. Lett. **94**, 175301 (2005).
[6] C. Josserand, Y. Pomeau, and S. Rica, Phys. Rev. Lett. **98**, 195301 (2007).
[7] S. M. Roccuzzo and F. Ancilotto, Phys. Rev. A **99**, 041601(R) (2019).
[8] L. Tanzi, S. M. Roccuzzo, E. Lucioni, F. Famà, A. Fioretti, C. Gabbanini, G. Modugno, A. Recati, and S. Stringari, Nature **574**, 382 (2019).
[9] M. Guo, F. Böttcher, J. Hertkorn, J.-N. Schmidt, M. Wenzel, H. P. Büchler, T. Langen, and T. Pfau, Nature **574**, 386 (2019).
[10] G. Natale, R. M. W. van Bijnen, A. Patscheider, D. Petter, M. J. Mark, L. Chomaz, and F. Ferlaino, Phys. Rev. Lett. **123**, 050402 (2019).
[11] L. Tanzi, J. G. Maloberti, G. Biagioni, A. Fioretti, C. Gabbanini, and G. Modugno, arXiv:1912.01910.
[12] M. R. Matthews, B. P. Anderson, P. C. Haljan, D. S. Hall, C. E. Wieman, and E. A. Cornell, Phys. Rev. Lett. **83**, 2498 (1999).
[13] K. W. Madison, F. Chevy, W. Wohlleben, and J. Dalibard, Phys. Rev. Lett. **84**, 806 (2000).
[14] J. R. Abo-Shaeer, C. Raman, J. M. Vogels, and W. Ketterle, Science **292**, 476 (2001).
[15] P. C. Haljan, I. Coddington, P. Engels, and E. A. Cornell, Phys. Rev. Lett. **87**, 210403 (2001).
[16] M. W. Zwierlein, J. R. Abo-Shaeer, A. Schirotzek, C. H. Schunck, and W. Ketterle, Nature **435**, 1047 (2005).
[17] S. M. Roccuzzo, A. Gallemí, A. Recati, and S. Stringari, Phys. Rev. Lett. **124**, 045702 (2020).
[18] A. R. P. Lima and A. Pelster, Phys. Rev. A **86**, 063609 (2012).
[19] F. Wächtler and L. Santos, Phys. Rev. A **93**, 061603(R) (2016).
[20] R. Schützhold, M. Uhlmann, Y. Xu, and U. R. Fischer, Int. J. Mod. Phys. B **20**, 3555 (2006).
[21] H. Saito, J. Phys. Soc. Jpn. **85**, 053001 (2016).
[22] D. S. Petrov, Phys. Rev. Lett. **115**, 155302 (2015).
[23] C. R. Cabrera, L. Tanzi, J. Sanz, B. Naylor, P. Thomas, P. Cheiney, and L. Tarruell, Science **359**, 301 (2018).
[24] P. Cheiney, C. R. Cabrera, J. Sanz, B. Naylor, L. Tanzi, and L. Tarruell, Phys. Rev. Lett. **120**, 135301 (2018).
[25] G. Semeghini, G. Ferioli, L. Masi, C. Mazzinghi, L. Wolswijk, F. Minardi, M. Modugno, G. Modugno, M. Inguscio, and M. Fattori, Phys. Rev. Lett. **120**, 235301 (2018).
[26] G. Ferioli, G. Semeghini, L. Masi, G. Giusti, G. Modugno, M. Inguscio, A. Gallemí, A. Recati, and M. Fattori, Phys. Rev. Lett. **122**, 090401 (2019).
[27] L. Santos, G. V. Shlyapnikov, and M. Lewenstein, Phys. Rev. Lett. **90**, 250403 (2003).
[28] A. Recati, F. Zambelli, and S. Stringari, Phys. Rev. Lett. **86**, 377 (2001).
[29] K. W. Madison, F. Chevy, V. Bretin, and J. Dalibard, Phys. Rev. Lett. **86**, 4443 (2001).
[30] M. Abad, M. Guilleumas, R. Mayol, M. Pi, and D. M. Jezek, Phys. Rev. A **79**, 063622 (2009).
[31] D. H. J. O'Dell and C. Eberlein, Phys. Rev. A **75**, 013604 (2007).
[32] Y. Cai, Y. Yuan, M. Rosenkranz, H. Pu, and W. Bao, Phys. Rev. A **98**, 023610 (2018).
[33] A. J. Leggett, Phys. Rev. Lett. **25**, 1543 (1970).
[34] L. Pitaevskii and S. Stringari, *Bose-Einstein Condensation and Superfluidity* (Oxford University Press, Oxford, 2016).
[35] S. Sinha and Y. Castin, Phys. Rev. Lett. **87**, 190402 (2001).
[36] S. Stringari, Phys. Rev. Lett. **77**, 2360 (1996).
[37] R. M. W. van Bijnen, D. H. J. O'Dell, N. G. Parker, and A. M. Martin, Phys. Rev. Lett. **98**, 150401 (2007).

[38] T. Macrì, F. Maucher, F. Cinti, and T. Pohl, Phys. Rev. A **87**, 061602 (2013).

[39] Aside from the timescale on which the dynamics occurs, the final results and our conclusions do not change if instead of a step function we use, e.g., a linear ramp for $\Omega(t) \propto t$.

[40] See Supplemental Material at http://link.aps.org/supplemental/10.1103/PhysRevA.102.023322 for the full movie of the vortex nucleation, full dynamics of the vortex expansion and full dynamics of the vortex lattice expansion.

[41] N. G. Parker and C. S. Adams, Phys. Rev. Lett. **95**, 145301 (2005).

[42] It is important to note that in spite of the fact that the vortex core can be much larger in the dipolar case than in the more standard Bose condensates with only contact interaction (see Fig. 2), the number of vortices is independent of their size, being fixed by the value of the rotation frequency.

[43] H. Pu, L. O. Baksmaty, S. Yi, and N. P. Bigelow, Phys. Rev. Lett. **94**, 190401 (2005).

[44] J. W. Reijnders and R. A. Duine, Phys. Rev. A **71**, 063607 (2005).

[45] T. Sato, T. Ishiyama, and T. Nikuni, Phys. Rev. A **76**, 053628 (2007).

[46] D. S. Goldbaum and E. J. Mueller, Phys. Rev. A **79**, 063625 (2009).

[47] S. Tung, V. Schweikhard, and E. A. Cornell, Phys. Rev. Lett. **97**, 240402 (2006).

[48] F. Ancilotto, M. Barranco, M. Pi, and L. Reatto, Vortices in the Supersolid Phase of Dipolar Bose-Einstein Condensates, arXiv:2002.05934.